ACS APPLIED MATERIALS & INTERFACES

Functional Nanostructured Materials (including low-D carbon)

Hydrogen peroxide-assisted ultrasonic synthesis of BCNO QDs for the anthrax biomarker detection

Mingcong Rong, Xiaohua Yang, Longzhen Huang, Siting Chi, Youbin Zhou, Yune Shen, Buyun Chen, Xiangzhou Deng, and Zhao-Qing Liu

ACS Appl. Mater. Interfaces, **Just Accepted Manuscript** • DOI: 10.1021/acsami.8b21786 • Publication Date (Web): 21 Dec 2018

Just Accepted

ACS Publications

is published by the American Chemical Society. 1155 Sixteenth Street N.W., Washington, DC 20036

Hydrogen peroxide-assisted ultrasonic synthesis of BCNO QDs for the anthrax biomarker detection

Mingcong Rong[1*], Xiaohua Yang[1], Longzhen Huang[1], Siting Chi[1], Youbin Zhou[1], Yune Shen[1], Buyun Chen[2], Xiangzhou Deng[1], Zhao-Qing Liu[1*]

[1]*School of Chemistry and Chemical Engineering, Guangzhou University, Guangzhou 510006, China*

[2]*GuangDong Women and Children Hospital, Guangzhou 510010, China*

ABSTRACT: A facile 3% hydrogen peroxide-assisted ultrasonic synthetic strategy is demonstrated to successfully synthesize fluorescent boron carbon oxynitride quantum dots (BCNO QDs). The obtained BCNO QDs exhibit intense blue fluorescence, favorable biocompatibility and water-solubility. The quantum yield of the BCNO QDs is 19.9%. Owing to the absorbance energy transfer emission effect, an efficient ratiometric fluorescence biosensor is developed for the anthrax biomarker detection based on the BCNO QDs-EDTA-Eu^{3+} complex. Under optimal conditions, the detection limit of the anthrax biomarker is 0.5 nM. Furthermore， the sensitivity of the system was evaluated by *B. subtilis* spores and as low as 1.95×10^6 spores was detected. Combined a smartphone with the home-made BCNO QDs test paper, the lowest recorded visual detection limit of 1.0 μM anthrax biomarker was achieved when using a portable UV lamp. The fast response speed, excellent sensitivity and selectivity of the approach show potential applications in clinical analysis.

KEYWORDS: BCNO QDs; 2,6-dipicolinic acid (DPA); Ratiometric fluorescence biosensor; Fluorescence test paper; the AETE effect

INTRODUCTION

As a typical rare earth-free boron nitride (BN) based luminescence material, bulk boron carbon oxynitride (BCNO) phosphors have attracted extensive attentions owing to their nontoxicity, high quantum efficiency and tunable emission wavelength via adjusting carbon content or calcination temperature.[1-6] In recent years, many strategies have been developed to regulate and optimize their luminescence mechanism, such as the closed-shell BO^- and BO^{2-} anions-derived emission,[7] electron transition from nitrogen vacancy-induced emission which stems from carbon and oxygen impurity doping,[8] intrinsic state emission and surface defect state emission.[9] However, the controlled synthesis and large-scale application of BCNO nanomaterial are still at the initial stage of development. For example, BCNO nanosheets prepared by ultrasonic stripping with a sonic tip of bulk BCNO have been used in Cu^{2+} detection.[10] BCNO QDs obtained from ammonium hydroxide hydrothermal method have been applied in bioimaging.[11] BCNO nanocrystals obtained from soaking the bulk BCNO in water are aggregations of particles. The poor dispersion hampers their application in chemical sensing.[4] SBA-15 template method have been used to gain BCNO QDs and applied in heavy metal ions detection.[12] Though some progress has been made in this regard, it is imperative to develop the more facile and feasible synthesis methods, and further promote the applications of the versatile BCNO QDs.

Bacillus anthracis (*B. anthracis*) is a kind of spore-forming harmful bacteria, which is prevalent in soil and plants and can be easily transferred to meat and dairy products. Since being used as a potential bioterrorism in the U.S. in 2001, sensitive detection of *B. anthracis* spores has become highly indispensable.[13] Inhalation of over 10^4 *B. anthracis* spores is lethal without timely medical treatment within 36 h.[14] Since 2, 6-dipicolinic acid (DPA) accounts 5-15% of the dry mass of the bacterial spores, it becomes a typical anthrax biomarker.[15] Consequently, it's vital to develop prompt, sensitive and accurate detection methods for DPA. Currently, popular techniques for quantitative analysis of DPA include surface-enhanced Raman scattering,[16-18] ratiometric colorimetric method[19] and ratiometric fluorescence method[14,20,21]. Among of those techniques, the ratiometric fluorescence method shows a lower detection limit, faster and more sensitive response to DPA. Notably, the lanthanide ion-based ratiometric fluorescence sensors for DPA detection have aroused considerable interests owing to the bright lanthanide ions luminescence, narrow emission peaks, large stokes shifts, long luminescence lifetime and high accuracy.[15]

Herein, we present a simple ultrasonic synthesis strategy to design and fabricate the fluorescent BCNO QDs. Coordinated with EDTA and Eu^{3+} ions, the blue fluorescence of BCNO QDs was used as a reference of the fluorescence signal. By adding the DPA, it would coordinate with the BCNO QDs-EDTA-Eu^{3+} complex, the fluorescence of Eu^{3+} was activated and a bright red fluorescence detection signal appeared. Inspired by the absorbance energy transfer emission (AETE) effect derived from Eu^{3+}-DPA complex, an effective ratiometric fluorescence sensor for the anthrax biomarker DPA detection has been further fabricated. The proposed approach shows two linear ranges from 0 to 700 nM and 700 nM to 2.5 μM, with a detection limit of 0.5 nM. Moreover， the sensitivity of the system was evaluated by *B. subtili*s spores and with the detection limit of 1.95×10^6 spores was detected. In addition, BCNO QDs test paper was fabricated and a lowest recorded visual detection limit of 1.0 μM DPA was obtained when using a 254 nm UV lamp. This work aims to develop a convenient background-free and self-calibrating method for fast and sensitive analysis of the DPA.

EXPERIMENTAL SECTION

Chemicals and Reagents.

Boric acid, urea, ethylenediamine tetraacetic acid disodium salt (EDTA) and europium nitrate hexahydrate were purchased from Aladin Ltd. (Shanghai, China). Polyethylene glycol (PEG, Mw: 20k) was purchased from Alfa Aesar Ltd. (Shanghai, China). 2,6-dipicolinic acid (DPA), phthalate (PH), picolinic acid (PA), nicotinic acid (NA), isonicotinic acid (ISA) were purchased from Sigma-Aldrich, Inc. (U.S.). *Bacillus subtilis* (*B. subtilis*, CCTCC AB 90008) were purchased from China Center for Type Culture Collection (CCTCC, Wuhan, China). All chemicals used in the experiments were of analytical grade. Ultrapure water with a resistivity of 18.2 MΩ/cm was used in preparing solutions. Fiber filters were purchased from Sinopharm Chemical Reagent Co., Ltd (Shanghai, China).

Preparation of the bulk BCNO.

Bulk BCNO was prepared according to a previous report with some modification.[3] 0.02 mol boric acid (considered as B source), 0.05 mol urea (considered as N source), different amount of PEG (considered as the C source and remain the C/B molar ratio of 0.25, 0.50, 0.75, 1.0 and 1.5) were dissolved in 20 mL ultrapure water. After fully

stirred and concentrated, the solution was dried in the oven at 80°C. Then the white mixtures were transferred to a muffle furnace and calcined at 750°C for 1 h.

Preparation of the BCNO QDs.

BCNO QDs were prepared using bulk BCNO with the C/B molar ratio of 1.0. 20 mg bulk BCNO was added into 50 mL fresh 3% H_2O_2 solution. After continuous ultrasonic at 40 kHz for 3 h, the turbid solution turned into transparent yellowish solution. Filtered through a 0.22 μm water phase microporous membrane filter, blue fluorescent BCNO QDs were obtained. The concentration of the as-prepared BCNO QDs was estimated to be 400 μg/mL.

Ratiometric fluorescence sensing of DPA.

First, 50 μL EDTA (2 μM) and 50 μL europium nitrate solution (2 μM) were added into 100 μL BCNO QDs solution in sequence. Then the solution was added into Tris-HCl buffer (10 mM, pH 7.0) with different concentrations (0, 0.5, 2.5, 5, 10, 25, 50, 100, 150, 200, 300, 500, 700, 800, 900, 1000, 1500, 2000 and 2500 nM) of DPA. The final volume of the solution was kept at 1.0 mL. Fluorescence spectra were collected 10 min after adding the DPA. In the selectivity detection, the concentration of homologous compounds was 100 μM and the DPA concentration was 2.5 μM. Since the excitation wavelength appeared at ~270 nm, a 320 nm long pass filter has been applied to eliminate the excitation light.

The interaction mechanism between the BCNO QDs and DPA were investigated by time-resolved decay measurements. BCNO QDs were added into Tris-HCl buffer (10 mM, pH 7.0) with varying concentrations (0, 50, 500, 1000 and 2000 nM) of DPA. The other conditions were the same as above (excitation wavelength: 270 nm, emission wavelengths: 395 and 616 nm).

In the bacterial spore detection, the noninfectious analogue *B. subtilis* spores were used instead. The procedure were managed refer to the reported literature.[14] Sporulation of *B. subtilis* was incubation at 37°C for 3 days on an Lab 28 nutrient agar containing 10 g/L tryptone, 5 g/L yeast extract and 10 g/L NaCl. After sporulation, the spores were scraped from the agar plates and suspended in ultrapure water. The spores were washed five times with ultrapure water and centrifuged at 17000g for 5 min, ensuring the complete remove of culture medium. Then the spores were suspended in 1 mL alanine solution (10 mM) and maintained at 70°C in water bath for 1 h to activate the germination process and release DPA molecules. The spore number was estimated using the cytometry. In the detection of the released DPA, the

spore suspension was filtered through a 0.45 μm water phase microporous membrane filter to remove the bacteria and insoluble impurities. The fluorescence detection of released DPA (different amount of spore metabolites: 0, 3, 4, 5, 10, 25, 50, 100, 200, 300, 400, 500, 600 and 700 μL) was the same as above mentioned process. The final solution contains 50 μL EDTA (2 μM), 50 μL europium nitrate solution (2 μM) and 100 μL BCNO QDs. The final volume of the solution (10 mM, pH 7.0) was kept at 1.0 mL. The stock solution of the spore metabolites was estimated to be 6.5×10^8 spores/mL (±20%).

Cell imaging of the BCNO QDs with spiked DPA.

The detail cell imaging operation process was illustrated in the supplementary material.

The visual BCNO QDs test paper for DPA assay.

The BCNO QDs test paper was prepared according to a previous report.[15] Circular strips (diameter ca. 6 mm) were fabricated using commercial fiber filter paper by a hole puncher. 5 μL BCNO QDs-EDTA-Eu^{3+} complex (1.2 mg/mL) was added onto the circular strip and then dried naturally to obtain the BCNO QDs test paper. Then, 5 μL solution containing varying DPA concentrations (0, 1, 10, 50, 100, 150, 200, 300, 400 and 500 μM) was added onto the BCNO QDs test paper. In the DPA detection of real samples, water samples were collected from the Pearl River and Guangzhou University campus, then filtered through the 0.22 μm water phase membrane. Cell fragmentation fluid (CFF) was obtained from MCF-7 cells. 2 μL real samples were added along with the DPA solution, the remaining steps were the same as above. The fluorescence color of the BCNO QDs test paper is visible to the naked eye under a portable 254 nm UV lamp. The fluorescence photos were acquired using a smartphone. Subsequently, the concentrations of DPA could be quickly dertermined with a color-scanning app (Photoshop, Adobe). The detail operation process was illustrated in the supporting information (Scheme S1).

RESULTS AND DISCUSSIONS

The synthesis, characterization and properties of the bulk BCNO.

The bulk BCNO was synthesis by the high temperature combustion method. With the increase of the C/B molar ratio, the higher amount of carbon doping led to a darker color (from pale yellow to orange-yellow) of the bulk BCNO (Fig. S1). The morphology of the bulk BCNO was characterized by SEM. As shown in Figs. 1A-E,

the bulk BCNO with different C/B molar ratio exhibits an irregular bedded structure in sub micron size. The element compositions of the bulk BCNO revealed by EDX analysis show consistency with those of the raw materials (Figs. 1F and S1). All the bulk BCNO materials possess the similar BN typical structures according to the XRD, IR and XPS measurements (Figs. S2-4, details were illustrated in the supporting information). The absorption spectra of the bulk BCNO show a red-shift with higher C/B ratio (Fig. S5A), which is consistent with the color changes of bulk BCNO in Fig. S1. Together with the decreased fluorescence intensity of the bulk BCNO with increased C/B ratio (Fig. S5B), these results indicate the atomic scale incorporation of carbon and oxygen into the structure, which is in accordance with the previous report.[1] Carbon has been incorporated into the covalent framework of layered BN. B-O bonds on the more oxidation sensitive surface sites can be beneficial to the formation of BCNO. Obviously, the optimum fluorescence emission spectra of the bulk BCNO show a red-shift from 420 to 540 nm with higher C/B ratio (Fig. S6). The emission is mainly induced by the transitions from nitrogen vacancy levels caused by carbon and oxygen impurity levels. With the increase of carbon and oxygen source, the carbon-related levels become broader and result in the red-shift of absorption and emission of the bulk BCNO.[8]

The synthesis and characterization of the BCNO QDs.

Disperse the bulk BCNO into a 3% H_2O_2 solution. After continuous ultrasonic for 3 h, the turbid solution turned into a transparent yellowish solution. In contrast, the precipitation in the bottom of the flask barely diminished when put the bulk BCNO into ultrapure water under 3 h continuous ultrasonic reaction. So we speculated that some hydroxyl radicals were generated from H_2O_2 and cut the bulk BCNO into small BCNO QDs during the ultrasonic process.

The morphologies, elemental compositions and chemical bonding structure of the BCNO QDs were investigated. The BCNO QDs show a diameter ranging from 5.5 to 14.5 nm, with a mean size of 10.1 nm (Fig. 2A). Since the BCNO QDs indicate an extremely small crystalline size, they show a broad diffraction band ranging from 15° to 34° in Fig. 2B. As shown in Fig. 2C, two strong bands at 780 and 1385 cm^{-1} were ascribed to the in-plane stretching and out-of-plane bending vibrations of h-BN. The absorption bands at 925, 1024 and 1100 cm^{-1} were attributed to N-B-O, B-O-B and B-O bonds. Whereas, the abroad absorption bands around 1200 to 1600 cm^{-1} corresponded to B-N and C-N bonds.[1,6,22,23] In addition, the absorption bands at 3217

and 3373 cm^{-1} were assigned to N-H and O-H bands.[24,25] The XPS spectrum showed that the BCNO QDs consisted of B, C, N and O elements with a corresponding atomic ratio of 0.274:0.273:0.247:0.206 (Fig. S7). The B 1s spectrum displayed three peaks centered at 190.0, 190.9 and 192.4 eV, which were ascribed to B-C, B-N and B-O bonds. The C1s spectrum exhibited four peaks centered at 283.5, 284.8, 286.4 and 288.8 eV, which were attributed to C-B, graphitic carbon, C-N/C-O and C=N/C=O bonds. The N1s spectrum revealed three peaks centered at 398.4, 400.0 and 401.0 eV, which corresponded to N-B, C=N and C-NH bonds. The O1s spectrum showed two peaks centered at 531.9 and 532.8 eV, which were assigned to O-B and O-C bonds.[23,26,27] All the above results verified that the BCNO QDs kept the typical characteristics of the bulk BCNO. The hydrated ionic radius of the BCNO QDs is ~28 nm, indicating a good dispersibility in aqueous (Fig. S8). The BCNO QDs are negatively charged with the zeta potential of -35.6 mV (in water) and -46.3 mV (in the detection condition) (Fig. S9). The strongly negative surface charges originate from the superficial B-O and O-H units and account for the stability and favorable water-solubility of the BCNO QDs. The BCNO QDs maintained pale yellow clear solution for six months at room temperature, revealing their excellent stability.

Optical properties of the BCNO QDs.

The optical properties of the BCNO QDs were tested by UV-vis absorption and fluorescence spectra. Different from previous reports, the BCNO QDs prepared only show an absorption in the deep ultraviolet region without any obvious absorption bands (Fig. 3A). Two fluorescence excitation peaks centered at 290 and 345 nm are available to the fluorescence emission peak at 395 nm. A new fluorescence emission shoulder peak at 500 nm appears when excited at 345 nm. Not only the BCNO QDs obtained from bulk BCNO with the C/B molar ratio of 1.0 possess the unique optical properties, BCNO QDs derived from bulk BCNO with other C/B molar ratio have the similar fluorescence excitation and emission peaks (Fig. S10, for example). These results imply that in the exfoliation process of the bulk BCNO into BCNO QDs, there are two kinds of QDs. The 395 nm emission is mainly derived from the intrinsic state luminescence from the h-BN structure, and the 500 nm emission is induced by the transition from nitrogen vacancy luminescence origins from the carbon and oxygen doping. The fluorescence of the BCNO QDs shifted from blue to red bands after adding 60 μM DPA (the insert photo in Fig. 3A). This indicates the feasibility of the ratiometric fluorescence detection of DPA. In addition, the BCNO QDs exhibits an

excitation-dependent fluorescence behavior, which may be ascribed to the different sizes of the BCNO QDs (Fig. 3B). With quinine sulfate as reference, the quantum yield (QY) of the BCNO QDs was estimated to be 19.9% (Table S1). Finally, the effects of pH and salinity tolerance on the fluorescence intensity of the BCNO QDs were tested to obtain the proper analysis conditions. In addition, the BCNO QDs displayed a high salinity tolerance and the fluorescence intensity of the BCNO QDs maintained constant when the pH varied from 3 to 7. However, the fluorescence intensity decreased rapidly in alkaline conditions (Figs. S11 and S12). Additionally, the fluorescence intensity of the BCNO QDs decayed fast (75.8%) under continuous 1 h fluorescence irradiation (Fig. S13). Accordingly, the BCNO QDs were stored in a dark place. These results revealed the potential application of the BCNO QDs in rapid fluorescence detection under physiological conditions.

Cell imaging of the BCNO QDs.

Finally, the fluorescent BCNO QDs were used for the cell imaging application. The biocompatibility of the BCNO QDs was tested by evaluating the viability of the Hela cells using an MTT assay (Fig. S14). The cell viability remained higher than 90% under different concentration of the BCNO QDs, even when the concentration was up to 1 mg/mL. This revealed the favorable biocompatibility of the BCNO QDs. Consequently, 200 μg/mL BCNO QDs were used for cell imaging. The Hela cells incubated with the BCNO QDs maintained the normal cell morphology and activity. Blue fluorescence can be observed inside the cells incubated with the BCNO QDs (Fig. 4). The above results imply that the BCNO QDs have been internalized by the Hela cells, exhibiting the potential in fluorescence bioimaging application.

Ratiometric fluorescence detection of DPA by AETE effect.

Currently, colorimetric sensing has become a popular analysis method in chemical sensing due to its convenience, simplicity and obviousness.[28,29] Ratiometric fluorescence sensing is similar to colorimetric sensing, two distinct fluorescence emissions are visible to the naked eye under one same fluorescence excitation wavelength. Among various fluorescence sensing methods, ratiometric fluorescence is well known for its high sensitivity, background-free and self-calibrating performance.[15] In the determination of DPA, when the EDTA and Eu^{3+} were added into the BCNO QDs solution, the BCNO QDs-EDTA-Eu^{3+} complex would form immediately (Fig. 5). The BCNO QDs-EDTA-Eu^{3+} complex emits the blue fluorescence at 395 nm under excitation at 270 nm, since the coordinated water

molecules prefer to produce quenching effect on the fluorescence of Eu^{3+}. In the determination of DPA, the DPA is not only a tridentate ligand to Eu^{3+}, but also an "antennas molecular" which could absorb the excitation light at 270 nm (the absorbance of DPA is around 270 nm, Fig. S15). The water molecules were substituted by the DPA after the addition of DPA, the nonradiative quenching effect of water molecules was blocked. Simultaneously, the coordinated DPA molecules transferred the absorbed energy to Eu^{3+}, giving rise to the intense red fluorescence of the Eu^{3+} (an increased emission at 593 and 616 nm by more than several orders of magnitude, derived from $^5D_0$ to ^7F_J, J = 0, 1, 2 of Eu^{3+}).[20] Using the red fluorescence of DPA-sensitized Eu^{3+} at 616 nm and blue fluorescence of the BCNO QDs at 593 nm as the fluorescence response signal and reference signal, an effective ratiometric fluorescence sensing approach towards the DPA detection was developed. The red fluorescence signal appeared quickly after the DPA addition and the fluorescence intensity kept steady after 10 min (Fig. S16). As the DPA concentration increased, the fluorescence intensity of the sensitized Eu^{3+} increased while the fluorescence intensity of the BCNO QDs maintained unchanged. The fluorescence emission intensity ratio of the peaks at 616 nm to that of 395 nm increased along with the DPA concentration, showing two linear ranges from 0 to 700 nM and 700 nM to 2.5 μM, with a detection limit of 0.5 nM (Fig. 6A). Two linear equations were obtained: $F_{616nm/395nm} = 7.68\times10^{-4}[DPA] + 0.192$ (0-700 nM) and $F_{616nm/395nm} = 1.36\times10^{-3}[DPA] - 0.161$ (700 nM-2.5 μM), with correlation coefficients R of 0.999 and 0.995. In the lower concentration range (0-700 nM) of DPA, the DPA-sensitized Eu^{3+} ions are relatively less. The increased red fluorescence is relatively slower. In the higher concentration range (700 nM-2.5 μM) of DPA, there are more DPA-sensitized Eu^{3+} ions, the red fluorescence increased sharply due to the special fluorescence of lanthanide ions (fluorescence enhancement in several orders of magnitude). These results show comparablility with previous works on the DPA detection (Table S2). This method shows excellent selectivity over some homologous compounds as well (Fig. 6B). In addition, the detection mechanism was further explored using fluorescence time-resolved decay measurements. As shown in Figs. 6C and 6D, the lifetime of the BCNO QDs remained constant (around 4.5 ns when excited at 270 nm, single exponential fitting), while the lifetime of the fluorescence of Eu^{3+} gradually increased (from 10.65 to 301.7 μs). The results certified the detection mechanism of AETE effect from DPA to Eu^{3+} on the BCNO QDs-EDTA-Eu^{3+}-DPA complex.[15,20]

Noninfectious stimulant for *B. anthracis*, *B. subtilis* was used for the detection of DPA released from bacterial spores. As shown in Fig. 7A, with the increased addition of the spore metabolites (in accordance with the DPA concentration), the intensity of the red fluorescence of the sensitized Eu^{3+} increased immediately. However, the intensity of the fluorescence of the BCNO QDs remained unchanged. The fluorescence intensity ratio of $F_{616nm/395nm}$ increased linearly with the increased amount of spore metabolites from 0 to 700 μL. The detection limit is 3 μL (corresponding to 1.95×10^6 *B. subtilis* spores).

Visual determination of DPA using the BCNO QDs test paper.

Nowadays, developing simple and convenient test papers for DPA detection has received extensive attentions.[15,20] Herein, a portable and facile BCNO QDs test paper was prepared using commercial fiber filer paper by a hole puncher. As shown in Fig. 7B, the fluorescence color of the BCNO QDs test paper shifted from blue to red upon exposure to different DPA concentration. Coupling a smartphone, the red-green-blue (RGB) intensity data of the fluorescence imaging photos can be analyzed with a color-scanning app (Scheme S1). A linearity curve of $R/B = 1.67\times 10^{-3}[DPA] + 0.276$ was obtained for the DPA detection. The 1.0 μM detection limit was achieved. Additionally, the BCNO QDs test paper shows potential practical applications. The recoveries of the real samples spiked with DPA varied in the range of 85.1% ~ 125.0%, while the RSD was still below 5% (Table S3). The BCNO QDs test paper showed favorably high stability after being protected from light and storage in a dry place, since the results varied in a reasonable range (Table S4). This indicates a practicability in the future application of the BCNO QDs based test paper.

CONCLUSIONS

In summary, blue fluorescent BCNO QDs have been successfully prepared by using the facile 3% hydrogen peroxide-assisted ultrasonic method. The BCNO QDs display favorable water solubility and biocompatibility. Based on the AETE effect, a ratiometric fluorescence biosensor for the DPA detection was developed, with a lowest recorded detection limit of 0.5 nM. Additionally, the *B. subtili*s spores were detected by the proposed method with a detection limit of 1.95×10^6 spores. Finally, portable BCNO QDs based test paper was fabricated for the potential practical DPA detection application. A lowest visual detection limit of 1.0 μM DPA was obtained when using a 254 nm UV lamp. This work provides a novel synthesis strategy for

BCNO QDs and a new way for rapid and efficient detection for the anthrax biomarker.

ASSOCIATED CONTENT

Supporting information

The Supporting information provides the details of the characteristic measurements (XRD, FT-IR, XPS spectra), optical properties of BCNO QDs, the DPA detection conditions, the operation process during the visual DPA detection and the real sample DPA detection.

AUTHOR INFORMATION

Corresponding Author

*E-mail: rongmc@gzhu.edu.cn, lzqgzu@gzhu.edu.cn

ORCID

Mingcong Rong: 0000-0002-7453-8028, Zhao-Qing Liu: 0000-0002-0727-7809

Notes

The authors declare no competing financial interest.

ACKNOWLEDGEMENTS

This work was financially supported by Guangdong Natural Science Foundation (Grant No. 2017A030311016 and 2017A030310652), Major Scientific Project of Guangdong University (Grant No. 2017KZDXM059), Science and Technology Research Project of Guangzhou (Grant No. 201607010232 and 201804010117) and Guangzhou University's training program for excellent new-recruited doctors (YB201717).

REFERENCES

(1) Lei, W.; Portehault, D.; Dimova, R.; Antonietti, M. Boron carbon nitride nanostructures from salt melts: tunable water-soluble phosphors. *J. Am. Chem. Soc.* **2011,** *133* (18), 7121-7127.

(2) Wang, L.; Zhang, J.; Qu, B.; Wu, Q.; Zhou, R.; Li, D.; Zhang, B.; Ren, M.; Zeng, X. C. Mechanistic insights into tunable luminescence and persistent luminescence of the full-color-emitting BCNO phosphors. *Carbon* **2017,** *122*, 176-184.

(3) Ogi, T.; Kaihatsu, Y.; Iskandar, F.; Wang, W.N.; Okuyama, K. Facile synthesis of new full-color-emitting BCNO phosphors with high quantum efficiency. *Adv. Mater.*

2008, *20* (17), 3235-3238.
(4) Liu, X.; Ye, S.; Qiao, Y.; Dong, G.; Zhang, Q.; Qiu, J. Facile synthetic strategy for efficient and multi-color fluorescent BCNO nanocrystals. *Chem. Commun.* **2009,** (27), 4073-4075.
(5) Suryamas, A. B.; Munir, M. M.; Ogi, T.; Khairurrijal; Okuyama, K. Intense green and yellow emissions from electrospun BCNO phosphor nanofibers. *J. Mater. Chem.* **2011,** *21* (34), 12629.
(6) Zhang, X.; Lu, Z.; Liu, H.; Lin, J.; Xu, X.; Meng, F.; Zhao, J.; Tang, C. Blue emitting BCNO phosphors with high quantum yields. *J. Mater. Chem. C* **2015,** *3* (14), 3311-3317.
(7) Wang, W.N.; Ogi, T.; Kaihatsu, Y.; Iskandar, F.; Okuyama, K. Novel rare-earth-free tunable-color-emitting BCNO phosphors. *J. Mater. Chem.* **2011,** *21* (14), 5183.
(8) Zhang, X.; Li, L.; Lu, Z.; Lin, J.; Xu, X.; Ma, Y.; Yang, X.; Meng, F.; Zhao, J.; Tang, C.; McKittrick, J. Effects of carbon and oxygen impurities on luminescence properties of BCNO phosphor. *J. Am. Ceram. Soc.* **2014,** *97* (1), 246-250.
(9) Kang, Y.; Chu, Z.Y.; Ma, T.; Li, W.P.; Zhang, D.J.; Tang, X.Y. Red photoluminescence BCNO synthesized from graphene oxide nanosheets. *Optoelectronics Lett.* **2016,** *12* (1), 1-4.
(10) Liu, Q.; Jiang, P.; Pu, Z.; Asiri, A. M.; Al-Youbi, A. O.; Sun, X. BCNO nanoparticles: A novel highly efficient fluorosensor for ultrarapid detection of Cu^{2+}. *Sensor. Actuat. B-Chem.* **2014,** *194*, 492-497.
(11) Xue, Q.; Zhang, H.; Zhu, M.; Wang, Z.; Pei, Z.; Huang, Y.; Huang, Y.; Song, X.; Zeng, H.; Zhi, C. Hydrothermal synthesis of blue-fluorescent monolayer BN and BCNO quantum dots for bio-imaging probes. *RSC Adv.* **2016,** *6* (82), 79090-79094.
(12) Jia, X.; Li, L.; Yu, J.; Gao, X.; Yang, X.; Lu, Z.; Zhang, X.; Liu, H. Facile synthesis of BCNO quantum dots with applications for ion detection, chemosensor and fingerprint identification. *Spectrochim. Acta. A.* **2018,** *203*, 214-221.
(13) Cowcher, D. P.; Xu, Y.; Goodacre, R. Portable, quantitative detection of Bacillus bacterial spores using surface-enhanced Raman scattering. *Anal. Chem.* **2013,** *85* (6), 3297-3302.
(14) Gao, N.; Zhang, Y.; Huang, P.; Xiang, Z.; Wu, F. Y.; Mao, L. Perturbing tandem energy transfer in luminescent heterobinuclear lanthanide coordination polymer nanoparticles enables real-time monitoring of release of the anthrax biomarker from bacterial spores. *Anal. Chem.* **2018,** *90* (11), 7004-7011.
(15) Rong, M.; Liang, Y.; Zhao, D.; Chen, B.; Pan, C.; Deng, X.; Chen, Y.; He, J. A ratiometric fluorescence visual test paper for an anthrax biomarker based on functionalized manganese-doped carbon dots. *Sensor. Actuat. B-Chem.* **2018,** *265*, 498-505.
(16) Zhang, X.; Young, M. A.; Lyandres, O.; Van Duyne, R. P. Rapid detection of an anthrax biomarker by surface-enhanced Raman spectroscopy. *J. Am. Chem. Soc.* **2005,** *127* (12), 4484-4489.
(17) Zhang, X.; Zhao, J.; Whitney, A. V.; Elam, J. W.; Van Duyne, R. P. Ultrastable substrates for surface-enhanced Raman spectroscopy: Al_2O_3 overlayers fabricated by

atomic layer deposition yield improved anthrax biomarker detection. *J. Am. Chem. Soc.* **2006,** *128* (31), 10304-10309.
(18) Bai, X. R.; Zeng, Y.; Zhou, X. D.; Wang, X. H.; Shen, A. G.; Hu, J. M. Environmentally safe mercury(II) ions aided zero-background and ultrasensitive SERS detection of dipicolinic acid. *Anal. Chem.* **2017,** *89* (19), 10335-10342.
(19) Yilmaz, M. D.; Oktem, H. A. Eriochrome black T-Eu^{3+} complex as a ratiometric colorimetric and fluorescent probe for the detection of dipicolinic acid, a biomarker of bacterial spores. *Anal. Chem.* **2018,** *90* (6), 4221-4225.
(20) Rong, M.; Deng, X.; Chi, S.; Huang, L.; Zhou, Y.; Shen, Y.; Chen, X. Ratiometric fluorometric determination of the anthrax biomarker 2,6-dipicolinic acid by using europium(III)-doped carbon dots in a test stripe. *Mikrochim. Acta.* **2018,** *185* (3), 201.
(21) Luan, K.; Meng, R.; Shan, C.; Cao, J.; Jia, J.; Liu, W.; Tang, Y. Terbium functionalized micelle nanoprobe for ratiometric fluorescence detection of anthrax spore biomarker. *Anal. Chem.* **2018,** *90* (5), 3600-3607.
(22) Zhang, X.; Jia, X.; Liu, H.; Lu, Z.; Ma, X.; Meng, F.; Zhao, J.; Tang, C. Spectral properties and luminescence mechanism of red emitting BCNO phosphors. *RSC Adv.* **2015,** *5* (51), 40864-40871.
(23) López-Salas, N.; Ferrer, M. L.; Gutiérrez, M. C.; Fierro, J. L. G.; Cuadrado-Collados, C.; Gandara-Loe, J.; Silvestre-Albero, J.; del Monte, F. Hydrogen-bond supramolecular hydrogels as efficient precursors in the preparation of freestanding 3D carbonaceous architectures containing BCNO nanocrystals and exhibiting a high CO_2/CH_4 adsorption ratio. *Carbon* **2018,** *134*, 470-479.
(24) Rong, M.; Lin, L.; Song, X.; Zhao, T.; Zhong, Y.; Yan, J.; Wang, Y.; Chen, X. A label-free fluorescence sensing approach for selective and sensitive detection of 2,4,6-Trinitrophenol (TNP) in aqueous solution using graphitic carbon nitride nanosheets. *Anal. Chem.* **2015,** *87* (2), 1288-1296.
(25) Rong, M.; Lin, L.; Song, X.; Wang, Y.; Zhong, Y.; Yan, J.; Feng, Y.; Zeng, X.; Chen, X. Fluorescence sensing of chromium (VI) and ascorbic acid using graphitic carbon nitride nanosheets as a fluorescent "switch". *Biosens. Bioelectron.* **2015,** *68*, 210-217.
(26) Tripathi, N.; Yamashita, M.; Akai, T. Synthesis and improved emission characteristics of BCNO@silica composites. *J. Mater. Chem. C* **2014,** *2* (4), 622-625.
(27) Dwivedi, J.; Kumar, P.; Kedawat, G.; Gupta, B. K. New emerging rare-earth free yellow emitting 2D BCNO nanophosphor for white light emitting diodes. *New J. Chem.* **2015,** *39* (7), 5161-5170.
(28) Zeng, J. B.; Fan, S. G.; Zhao, C. Y.; Wang, Q. R.; Zhou, T. Y.; Chen, X.; Yan, Z. F.; Li, Y. P.; Xing, W.; Wang, X. D. A colorimetric agarose gel for formaldehyde measurement based on nanotechnology involving Tollens reaction. *Chem. Commun.* **2014,** *50* (60), 8121-8123.
(29) Zeng, J. B.; Cao, Y. Y.; Chen, J. J.; Wang, X. D.; Yu, J. F.; Yu, B. B.; Yan, Z. F.; Chen, X. Au@Ag core/shell nanoparticles as colorimetric probes for cyanide sensing. *Nanoscale* **2014,** *6* (17), 9939-9943.

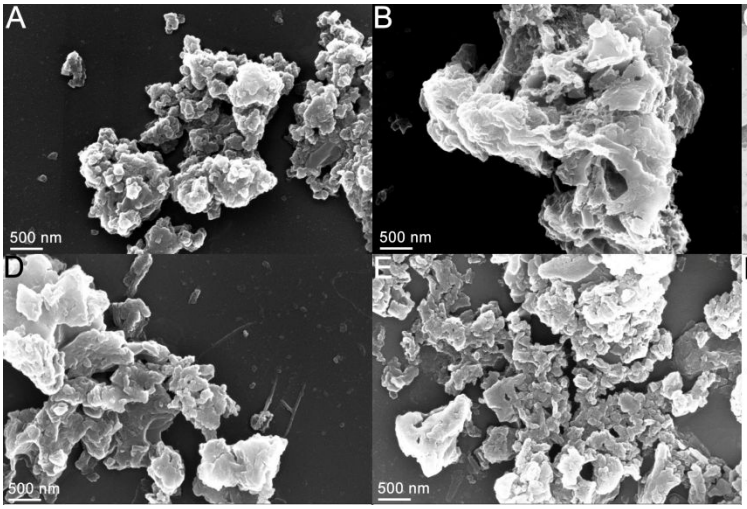

F

Table. The atom content of bulk BCNO by EDX spectrometric microanalysis with SEM

atom content/%	C/B: 0.25	C/B: 0. 50	C/B: 0.75	C/B: 1.0	C/B: 1.5
B	43.04	40.01	40.59	39.75	35.95
C	7.22	8.06	9.87	12.25	16.00
N	31.16	24.46	26.55	31.97	25.45
O	18.57	27.47	22.99	16.04	22.59

Fig. 1. SEM images of bulk BCNO with different C/B molar ratio. (A) 0.25, (B) 0.50, (C) 0.75, (D) 1.0, (E) 1.5, (F) the atom content of bulk BCNO determined by EDX spectrometric microanalysis with SEM.

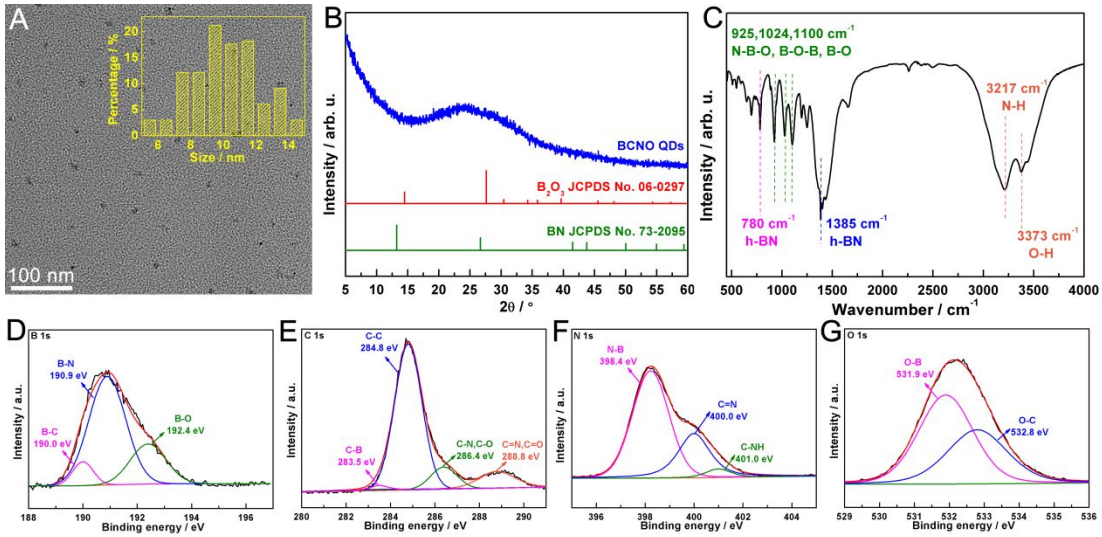

Fig. 2. (A) TEM image and size distribution of the BCNO QDs (inset). (B) XRD pattern, (C) FT-IR and (D-G) XPS spectra of the BCNO QDs.

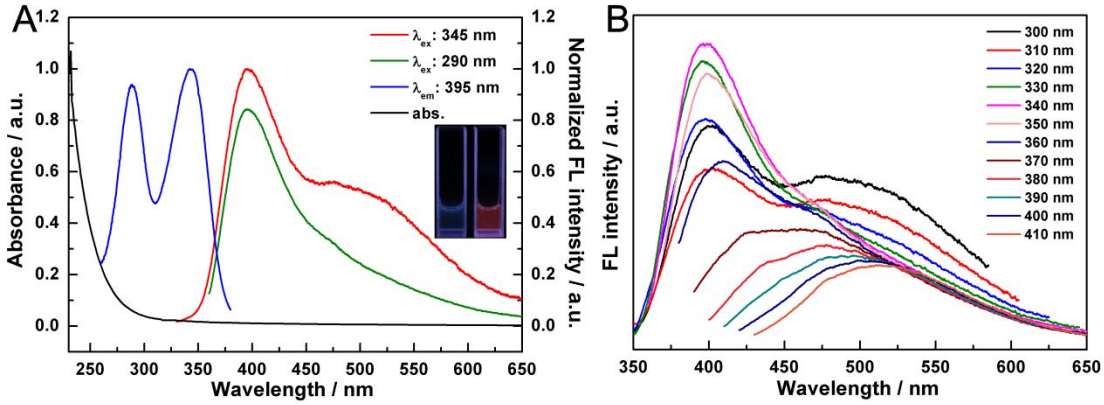

Fig. 3. (A) UV-vis absorption, fluorescence excitation and emission spectra of the BCNO QDs. Inset: the photograph of the BCNO QDs in the absence (left) and prescence (right) of 60 μM DPA under a 254 nm UV lamp. (B) The fluorescence emission spectra of the BCNO QDs with varying fluorescence excitation wavelengths.

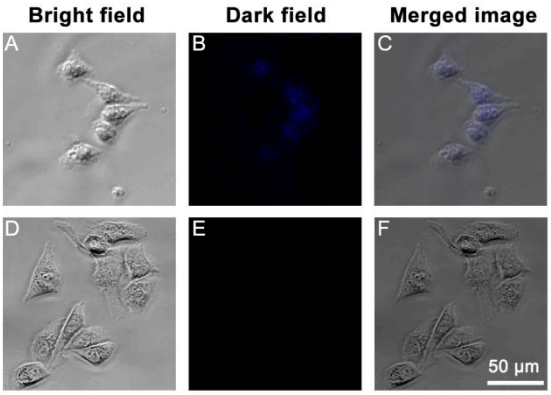

Fig. 4. Fluorescence graphs of the cultured cells. (A-C) HeLa cells incubated with the BCNO QDs for 6 h. (D-F) Control HeLa cells.

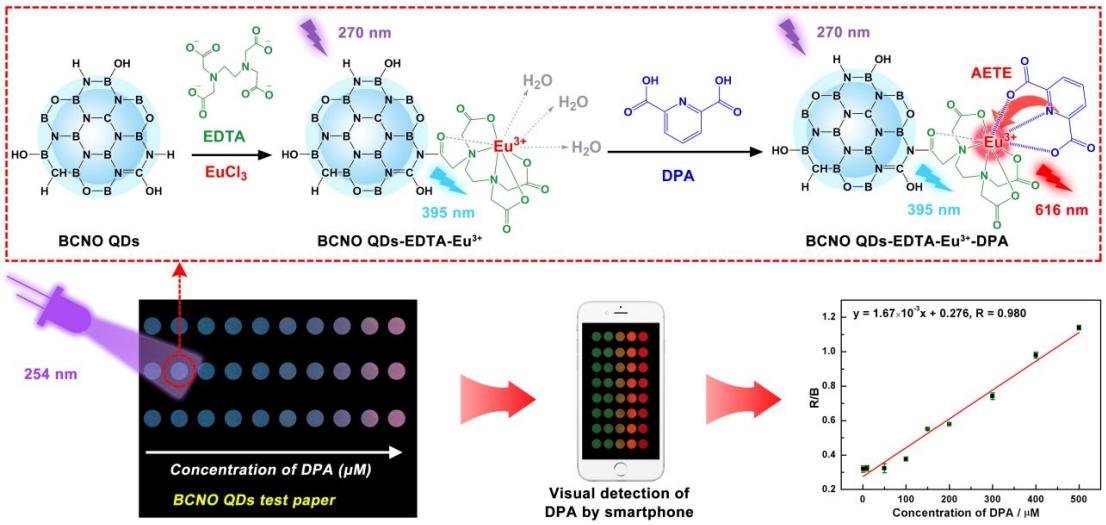

Fig. 5. Schematic illustration for DPA detection via the BCNO QDs based test paper.

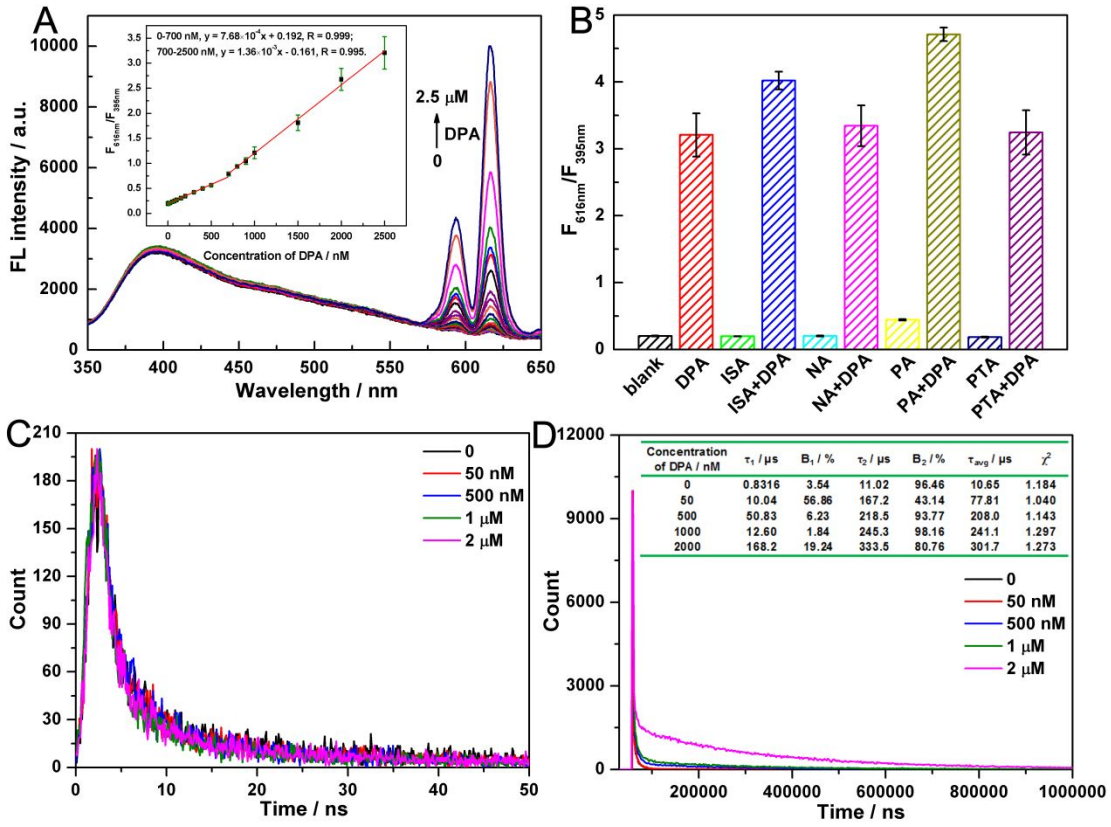

Fig. 6. (A) The fluorescence spectra of the BCNO QDs with respect to the DPA concentrations and the relationship between the ratio of $F_{616nm/395nm}$ and the DPA concentration (inset). (B) Fluorescence responses of the BCNO QDs in various interferents (100 μM) and in the absence/presence of DPA (2.5 μM, n=3). Time-resolved decay of fluorescence emission at (C) 395 nm, (D) 475 nm of the BCNO QDs-EDTA-Eu^{3+} system with different DPA concentrations. Inset: fluorescence emission lifetime at 616 nm of the BCNO QDs-EDTA-Eu^{3+} system with respect to the DPA concentrations.

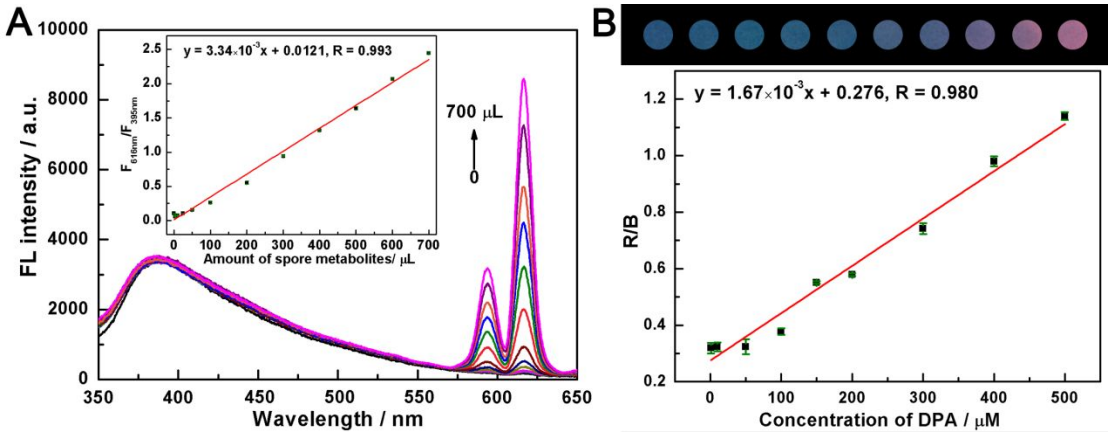

Fig. 7. (A) Fluorescence spectra of the BCNO QDs in different amount of spore metabolites of germinated *B. subtilis* spores. Inset: the relationship between the ratio of $F_{616nm/395nm}$ and the amount of the spore metabolites. (B) Fluorescence color images of the BCNO QDs test paper with different concentrations of DPA under a 254 nm UV lamp (above). The relationship between the intensity of R/B and DPA concentration (below).

Abstract Graphic

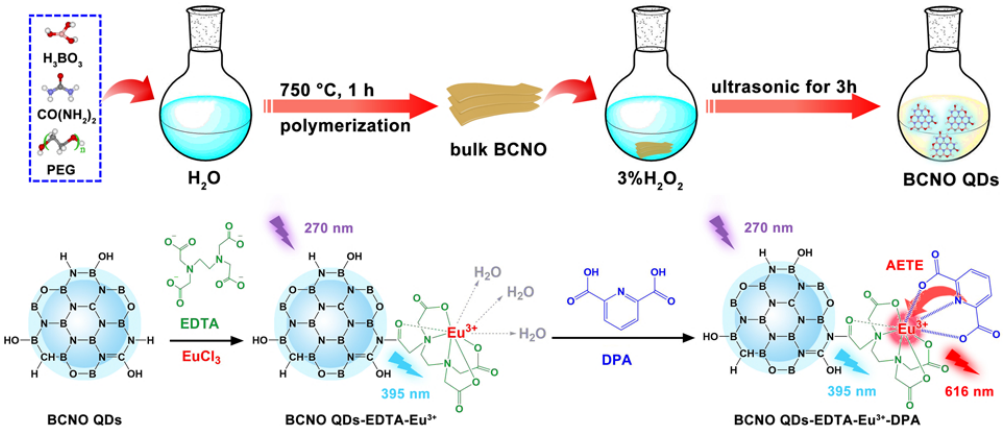

Table of content